DESIGN, FABRICATION AND DELIVERY OF AN IMPROVED SINGLE ELASTIC LOOP MOBILITY SYSTEM (ELMS)

Executive Summary Report

June 1972

HREC-7737-1
LMSC-HREC D225600-I

COPY NO.

LOCKHEED MISSILES & SPACE COMPANY

HUNTSVILLE RESEARCH & ENGINEERING CENTER

HUNTSVILLE RESEARCH PARK

4800 BRADFORD DRIVE, HUNTSVILLE, ALABAMA

DESIGN, FABRICATION AND DELIVERY OF AN IMPROVED SINGLE ELASTIC LOOP MOBILITY SYSTEM (ELMS)

Executive Summary Report

June 1972

Contract NAS8-27737

Prepared for National Aeronautics and Space Administration
Marshall Space Flight Center, Alabama 35812

by

W. Trautwein

APPROVED: T.R. Beal

T. R. Beal, Manager
Dynamics & Guidance Department

J. S. Farrior

J. S. Farrior
Resident Director

FOREWORD

This final report documents the results of a 10-month effort to finalize the design and fabricate an improved version of Lockheed's Elastic Loop Mobility System (ELMS). This effort was performed under Contract NAS8-27737 by Lockheed's Huntsville Research & Engineering Center for the National Aeronautics and Space Administration, George C. Marshall Space Flight Center (MSFC), Alabama, and it was sponsored by the Advanced Development Office, Advanced Manned Missions, NASA Headquarters. Dr. N. C. Costes of the Space Sciences Laboratory was the MSFC Contracting Officer's Representative (COR), with Mr. C. S. Jones, Jr., of the MSFC Astrionics Laboratory as the alternate COR.

Dr. W. Trautwein was the project engineer at Lockheed. He was assisted by Dr. C. J. Chang and Mr. G. P. Gill in engineering and design and by Mr. K. R. Leimbach in structural analysis.

Substantial support in manufacturing and metallurgical testing was obtained from the Process Engineering Laboratory's Research & Process Technology Division under Mr. W. Angele and, in particular, by Mssrs. J. R. Williams, P. G. Parks, E. A. Hasemeyer, V. H. Yost, and C. N. Irvine.

The assistance provided by Messrs. F. J. Nola and E. H. Berry of the Advanced Technology Branch, MSFC Astrionics Laboratory in providing high-performance electric drive motors and controllers for the test vehicle is gratefully acknowledged.

This report is divided into two volumes:

Volume I – Executive Summary Report
Volume II – Detailed Technical Report

Design details are documented in the form of engineering-type drawings, a reproducible set of which is submitted under this contract.

PROPRIETARY NOTICE

CONTENTS

Section 1
INTRODUCTION

The completion of a second-generation Elastic Loop Mobility System (ELMS) test unit under this contract represents an important step in the development of this new mobility concept for lunar and planetary roving vehicles which started three years ago as a Lockheed-funded project (Ref. 1). In 1970 a first-generation ELMS test unit was built under Company funds and tested at the U. S. Army Engineering Waterways Experiment Station (WES), Vicksburg, Mississippi, under NASA Defense Purchase Request No. H-74066A. The results from this NASA-MSFC sponsored test program (Ref. 2), directed by Dr. N. C. Costes of the Space Sciences Laboratory, showed improvement in performance over wheeled vehicles in the areas of slope climbing and obstacle negotiation with higher potential efficiencies in soft-soil traction. There was evidence that the ELMS concept could combine the advantage of tracked vehicles in all-terrain mobility without the conventional tracks' major shortcomings of high internal losses, mechanical complexity and heavy weight.

Based on lunar soil mechanics and wheel-soil interaction data obtained from the Apollo missions (Refs. 3 through 13), several significant design improvements were conceived during the development and testing of the first-generation ELMS and reduced to practice in the form of small-scale models as outlined in Refs. 14 and 15.

It was the objective of this contract to provide a full-scale ELMS test unit which would incorporate all the recent design improvements for later integration into a manned or unmanned articulated vehicle. A typical automated three-loop configuration is shown in Fig. 1. A single elastic loop front unit in tandem with a rear unit support by two elastic loops (arranged side by side) provides a high degree of mobility in roughest terrain if the two units are connected by articulated pitch and yaw joints. Major advantages of such an ELMS roving vehicle over wheeled designs are:

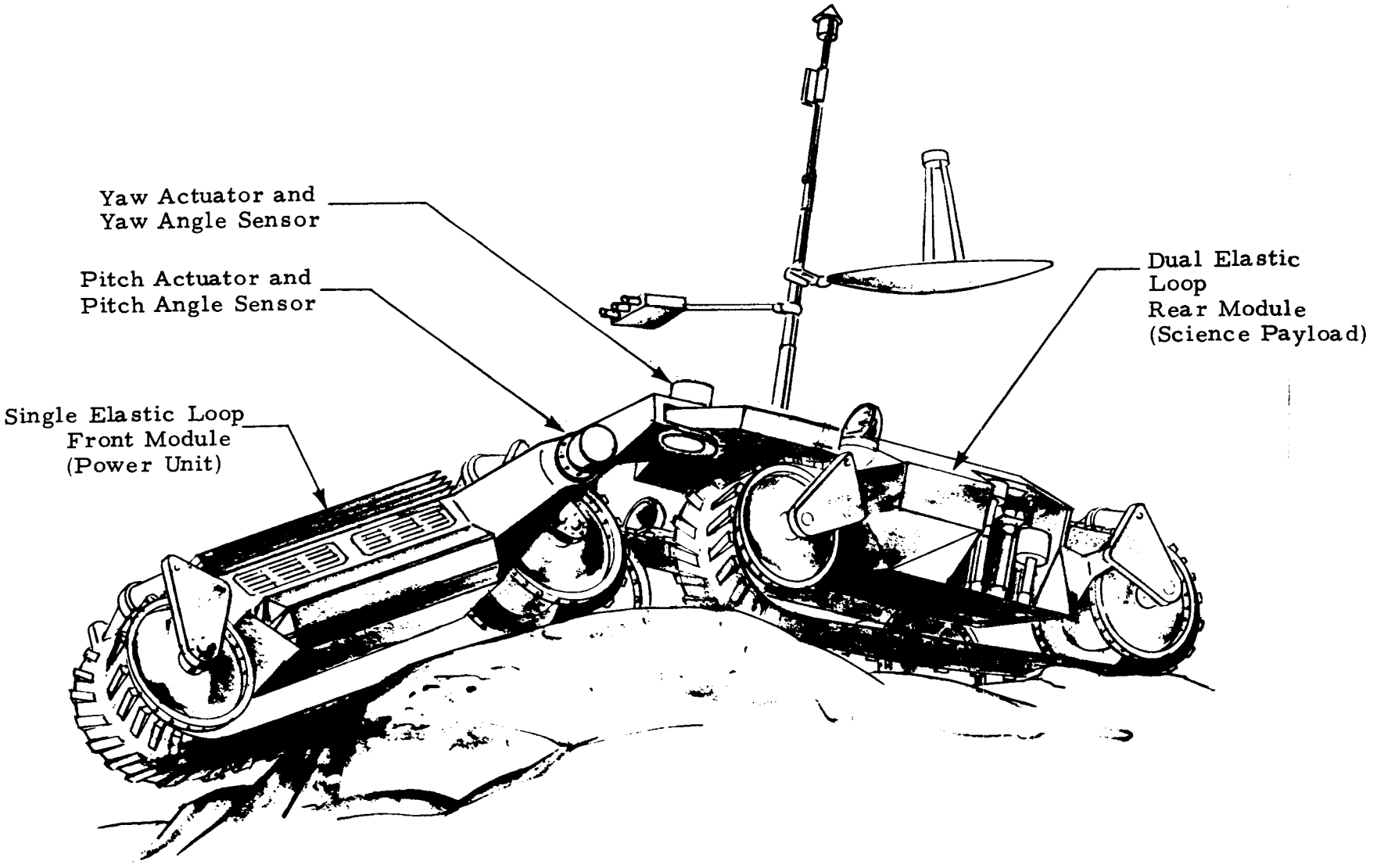

Fig. 1 - Typical Autonomous Rover Configuration Based on Lockheed's Elastic Loop Mobility System

- High static stability through low c.g. location.
- Better traction in soft soil which results in better slope climbing capability.
- Reduced drive torque requirements for obstacle negotiation.
- Simpler stowage, deployment concept and overall vehicle design.
- Smoother ride characteristics due to the large footprint.

The single-loop test unit built under this contract was to be supported and instrumented such that maximum realism could be obtained in its operation simulating the performance of multi-loop articulated vehicles.

The second-generation ELMS unit which was built under this contract is shown in Fig. 2a. Compared with the first-generation of Fig. 2b, the following major improvements have been incorporated:

- Redesign and manufacturing of elastic loop shape and size for uniform ground pressure distribution and higher load capability.
- Drive system modification for higher efficiency and torque requirements.
- Installation of large grousers for improved traction.
- Adjustable shock absorbers to optimize ELMS damping characteristics.
- Support trailer development for multi-mode operations, ranging from perfectly rotation-free hinge to perfectly rigid connection.
- Installation of extensive instrumentation of unambiguous ELMS performance testing.

In Section 2 these improvements are described in more detail. In Section 3 preliminary performance characteristics from recent acceptance tests at the WES are presented. A summary and conclusions and recommendations are given in Section 4 of this report.

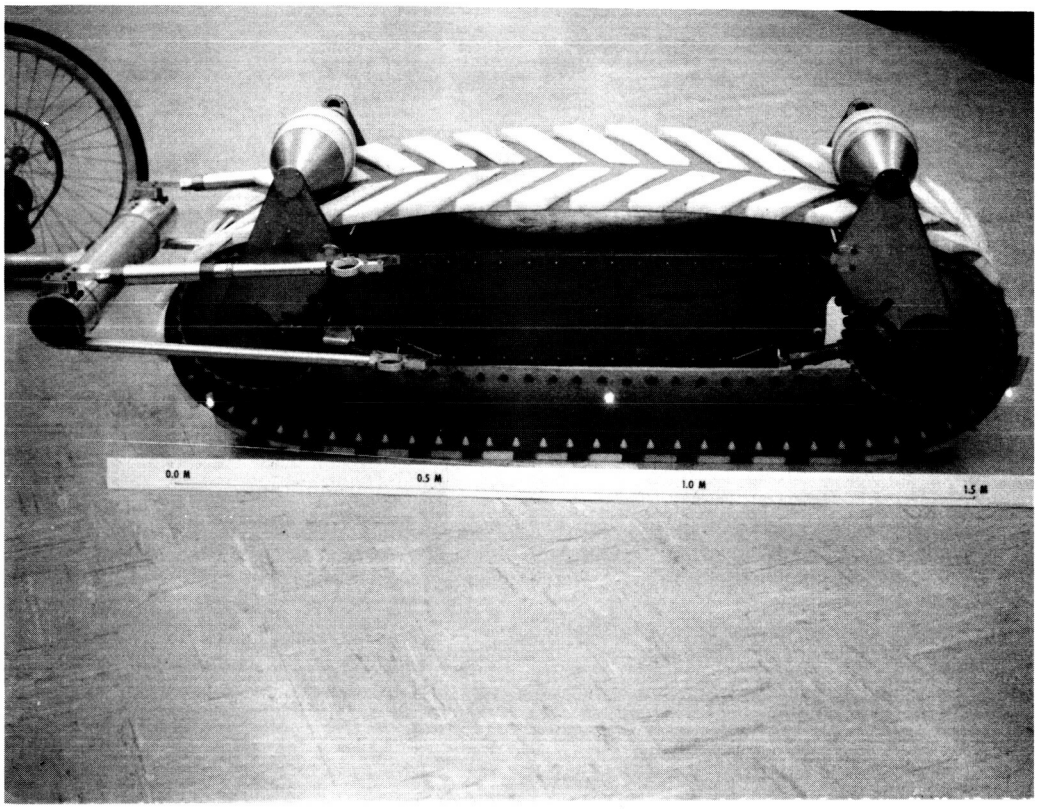

Fig. 2a - Second-Generation ELMS Test Unit Built Under Contract NAS8-27737 Features Uniform Ground Pressure Distribution (indicated by straight lower edge); large plastic grousers for improved traction; high load capability up to 670 N (150 lb); high efficiency drive system with brushless DC-motors (GFE); onboard battery power; telemetry and remote-control system, and instrumentation for performance evaluation.

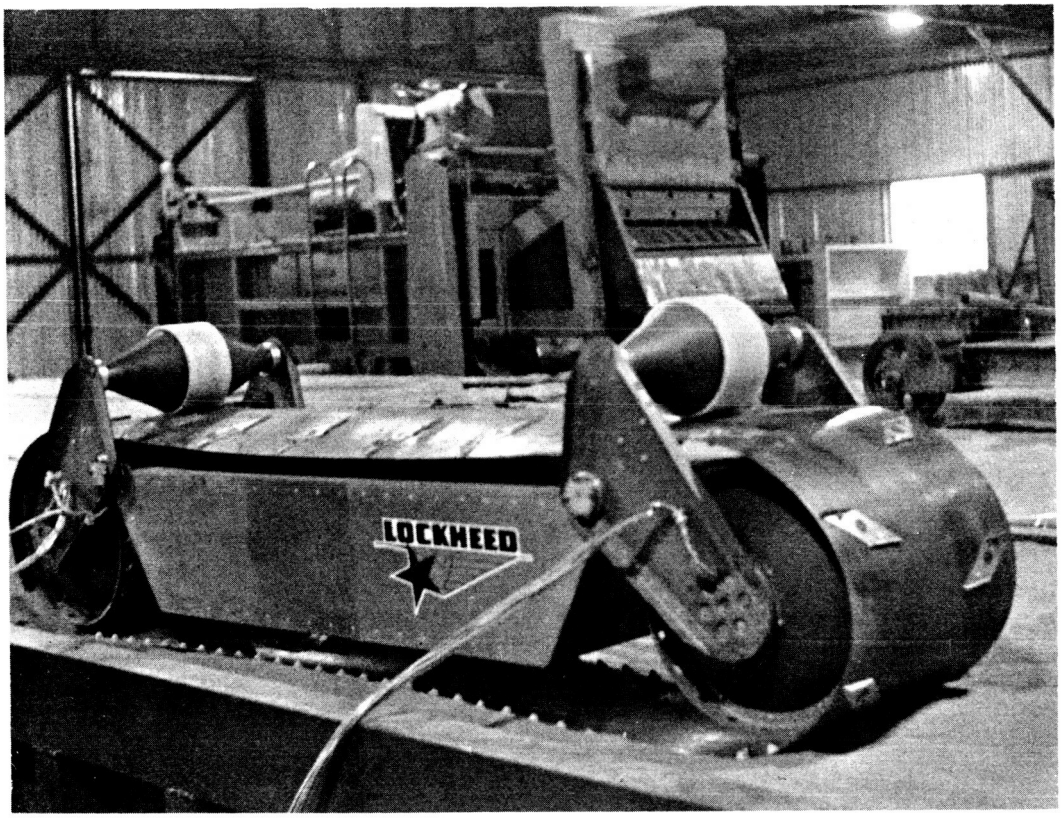

Fig. 2b - First-Generation ELMS Unit (1970) Exhibiting Low Load Carrying Capability of 253 N (57 lb) and High Non-Uniform Ground Pressure Distribution (indicated by curved lower edge).

Section 2
MAJOR DESIGN IMPROVEMENTS

2.1 ELASTIC LOOP REDESIGN FOR UNIFORM GROUND PRESSURE DISTRIBUTION AND INCREASED LOAD CAPABILITY

The previous loop manufacturing technique caused a substantial longitudinal curvature of the edge sections along the straight loop segments as shown in Fig. 2b. As a result, the loop sinkage into the soil and the contact pressure varies along the footprint with regions of high pressure fore and aft and low or zero pressure in the mid sections, which has adverse effects on soft soil performance. These earlier loops were manufactured by roll-forming a welded ring of a standard titanium alloy (Ti-6Al-4V).

The new loop design and forming technique (Fig. 2a) results in almost straight edge sections along the footprint and near uniform pressure distribution. This new loop form makes it possible to mount large grousers on both sides of the loop, thus greatly increasing the contact area and soft-soil traction.

The initial loop design did not allow for installation of batteries or heavier and stronger drive motors in a 1-g environment, because the dead weight of the unit of Fig. 2b of 380 N (86 lb) already exceeded the nominal design load of 253 N (57 lb) for the loop. Thorough design tradeoff studies and stress analyses have resulted in an increase in load capability of over 100% of the new elastic loop at an 11% increase in weight. The new ELMS test unit as shown in Fig. 2a weighs 510 N (115 lb) and accommodates 13 cm (5 in.) of spring deflection between chassis bottom and loop for dynamic loads and/or higher static load. This compares with only 7 cm (2.7 in.) available spring travel at 253 N (57 lb) for the first-generation ELMS of Fig. 2b. Selection of a more advanced titanium alloy keeps the maximum expected stress level below 33% of the strength at the weld joint. In the following section the major tools and manufacturing techniques are described, which were developed to obtain an elastic loop with uniform ground pressure distribution and higher load-carrying capability.

2.1.1 Loop Manufacturing Process

In Table 1 the major manufacturing steps to build the first and second generation elastic loops are summarized.

A standard annealed titanium alloy was used for the first-generation loop of Fig. 2b. After welding the sheet into a ring form and trimming to width the only forming operation was performed in the specially built single-stand roll-forming machine of Fig. 3. A set of three rolls bends the loop uniaxially at the location of the lower roll. By gradually moving the three rolls laterally across the entire width of the loop, a near-uniform transverse curvature is achieved. The resulting loop shape is characterized by upper and lower straight sections which are stiffened by the transverse curvature. The two flattened 180-degree sections can be used to provide spring suspension for the vehicle. The major shortcoming of first-generation loops can be observed in Fig. 2b: The edges are cambered along the straight sections. The resulting ground pressure distribution varies substantially along the footprint with high pressure regions fore and aft and low or zero pressure in the mid section near the edges. Thus, major areas of the loop's footprint are not contributing to the tractive effort.

A new loop form was developed (Refs. 14 and 15) which results in more uniform ground pressure distribution and therefore improved mobility in soft soil. As listed in Table 1 second-generation loops require a bulge-forming operation in addition to the uniaxial bending as obtained from the roll-former of Fig. 3 or from brake-bending the unwelded sheet as applied in the manufacture of small-scale models which do not require heat treatment.

The full size elastic loop built under this contract is made of a new titanium alloy to increase the load carrying capability. Best physical material characteristics are achieved by age hardening the welded loop under controlled conditions. The transverse curvature must then be formed after the age hardening imposing stringent requirements on the material.

Table 1

SUMMARY OF PAST AND PRESENT LOOP MANUFACTURING PROCESSES

Elastic Loop Model	First Generation Full Size (Fig. 2b)	Second Generation 1/6 Scale	Second Generation Full Size (Fig. 2a)
Material	Ti-6Aℓ-4V Annealed	Loops No. 1 and No. 2 and 1/6 Scale: Ti-11.5 Mo-6.5 Zr-4.6 Sn (Beta III) Loop No. 3: Ti-2Aℓ-11.5V-2Sn-11Zr (Transage 129)	
Manufacturing Step 1	TIG Weld Sheet into Ring Form 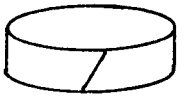	Brake-Bend Sheet for transverse curvature 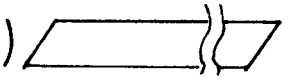	TIG-Weld Sheet into Ring Form 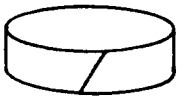
Step 2	Trim to Width (14 in.)	EB-Weld Strip into ring form 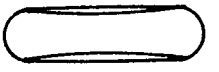	Trim to Width (16 in.)
Step 3	Roll-form for transverse curvature using Roll-former of Fig. 3 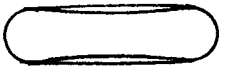	Bulge-form by trapped rubber process 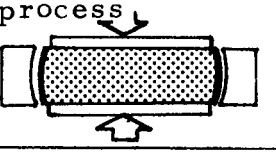	Bulge-form by hydraulic bladder process (Fig. 4) 
Step 4	Drill and assemble drive lugs and grousers	 Drill and assemble drive lugs and grousers	Age harden and descale
Step 5	—	—	Roll-form for transverse curvature using Roll-former of Fig. 3
Step 6	—	—	Drill and assemble drive lugs and grousers.

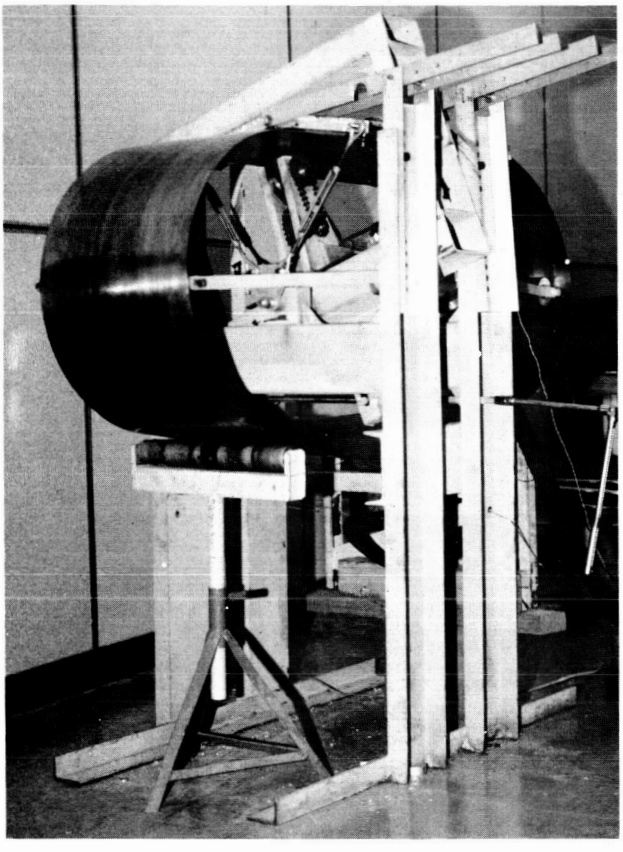

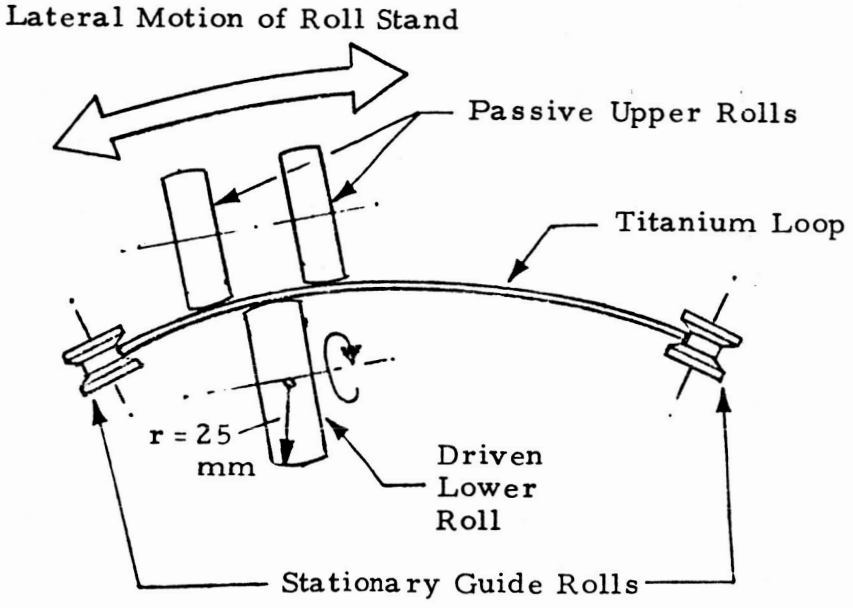

Fig. 3 - Single-Stand Roll-Forming Machine to Bend Transverse Curvature into Welded Elastic Loops Built Under Lockheed's Independent Development Program 1970.

For the bulge-forming of full size loops the tool shown in Fig. 4 was developed in cooperation with the Research and Process Technology Division of MSFC's Product Engineering Laboratory. Similar to the trapped-rubber forming process, which is used successfully in scale-model loop fabrication, the welded loop is pressed radially into an outer die whose inner wall is contoured to the desired bulge.

A waterfilled rubber bladder connected with a 1000 psi pump applies the radial pressure. During the bulge-forming the tool assembly is mounted onto the MSFC's Lake Erie press (MSFC No. 3994, Bldg. 4704), where a press load of 400 to 600 tons keeps the pressurized bladder chamber closed.

After bulge-forming (Step 3 in Table 1), the following operations are required to complete a second-generation elastic loop: age hardening; descaling; roll-forming; drilling and assembling drive lugs inside, the grousers outside.

Major difficulties which were encountered during the loop manufacture under this contract (discussed in detail in Vol. II, Section 2.4) were:

- Weld fracture in aluminum die for bulge-forming (welded by subcontractor). Die was repaired by bolting steel straps across the outer side of crack.
- Irregular bulge-form caused by partial binding of loop edge and upper plate due to vertical forces exerted by rubber bladder.
- Pinching of rubber bladder under high pressure, solved by protecting most vulnerable areas by fire hose material.
- Catastrophic failure of Beta-III-loop No. 2 during bulge-forming.
- Partial distortion of loops during age hardening, primarily due to larger-than-expected shrinkage of cold formed loops during heating. Transage 129 loop (No. 3) was distorted most since it required the highest age hardening temperature.
- Insufficient ductility of Beta III loops in age hardened weld sections for cold roll-forming. Loop No. 2 cracked over 6 inches near the end of the roll-forming operation and had to be repaired by welding the cracked portion.

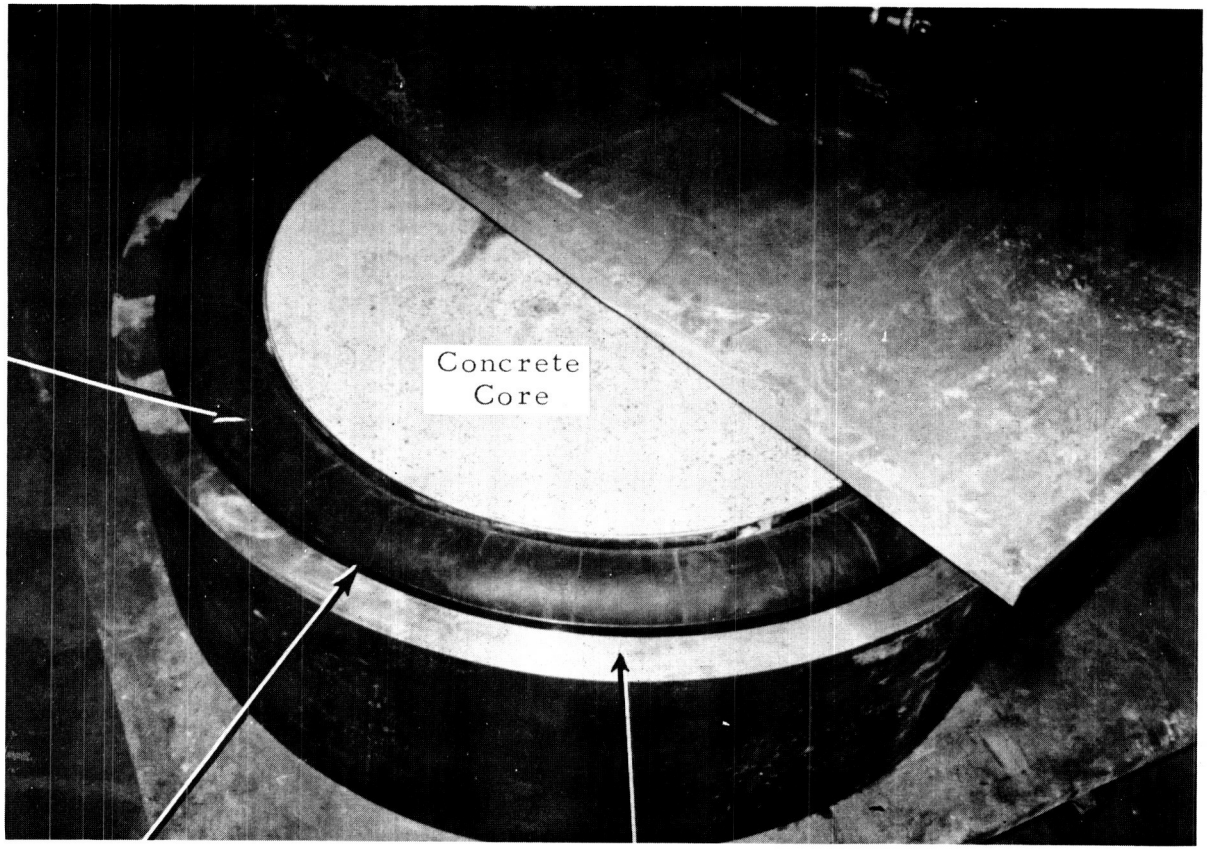

Water Filled Rubber Bladder

Aluminum Alloy Plates

Titanium Loop

Aluminum Die: Inner Wall Contoured to Desired Bulge Form

Fig. 4 - Bulge-Forming Tool for Elastic Loop Manufacturing

After all the forming operations on the three loops had been completed, loop No. 2 made of Beta III titanium alloy turned out to have the best performance characteristics and was selected. As indicated by the straight lower edges of the loop shown in Fig. 2a, the major objective of developing a uniform ground pressure distribution has been accomplished. This also resulted in a substantial performance improvement over the first-generation ELMS and over wheeled roving vehicles as indicated by the preliminary test results discussed in Section 3.

The experience gained in this loop manufacturing effort has led to an improved manufacturing technique which promises more uniform loops at reduced cost. A male hot-forming die sketched in Fig. 5 would combine the bulge-forming and age hardening operations. The large thermal expansion of the steel die with respect to the titanium loop plus the shrinkage of the sheet as received from the manufacturer would permit hot-forming the mild bulge of 15 m radius and removal from the die after aircooling, using a one-piece die.

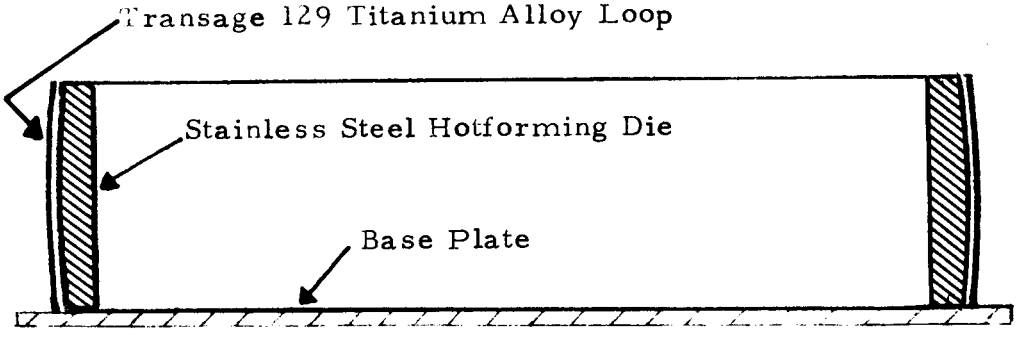

Fig. 5 - Proposed Manufacturing Techniques for Future Elastic Loops Combines Bulge-Forming and Age Hardening in One Simple Operation.

Small scale tests are planned to verify this approach.

2.2 DRIVE SYSTEM MODIFICATION FOR HIGHER EFFICIENCY AND TORQUE REQUIREMENTS

High performance brushless DC-drive motors have been provided by MSFC's Astrionics Laboratory as Government-furnished equipment (GFE) for the new ELMS drive system. They were incorporated into the internal drive drum design and form an integral part of the two drive drum and their suspension (Fig. 6). The total output torque of these motors of 216 N-m (160 ft-lb) is well above the torque requirements of the ELMS test unit. The maximum torque has, therefore, been limited to 81 N-m (60 ft-lb). This value represents the maximum expected torque required during obstacle negotiation and slope climbing. Sufficient torque will thus be available during the tests, whereas the first-generation ELMS drive system was torque-limited in a number of testing modes.

The two drive motors can satisfy stringent torque/speed requirements not achievable with minimum size permanent-magnet or series motors (Refs. 17, 18). High efficiency static controllers using pulse-width modulation were built and furnished as GFE by the Advanced Research and Technology Branch of the Astrionics Laboratory. Pulse-width modulation is used to minimize the problem of heat dissipation and to permit regenerative braking and continuous operation with full torque, if desired. The all solid-state controllers also affect winding shifts between series and parallel motor operation. This results in a 50% reduction in maximum controller current and a corresponding size and weight decrease.

The efficiency of the power transmission from the inner drive drums to the elastic loop was significantly improved by mounting arrays of planetary rollers around the drive drums (Fig. 7) eliminating sliding friction during engagement and disengagement of the drive lugs mounted along the loop. Frictionless flexural pivots have been used to minimize internal energy losses of

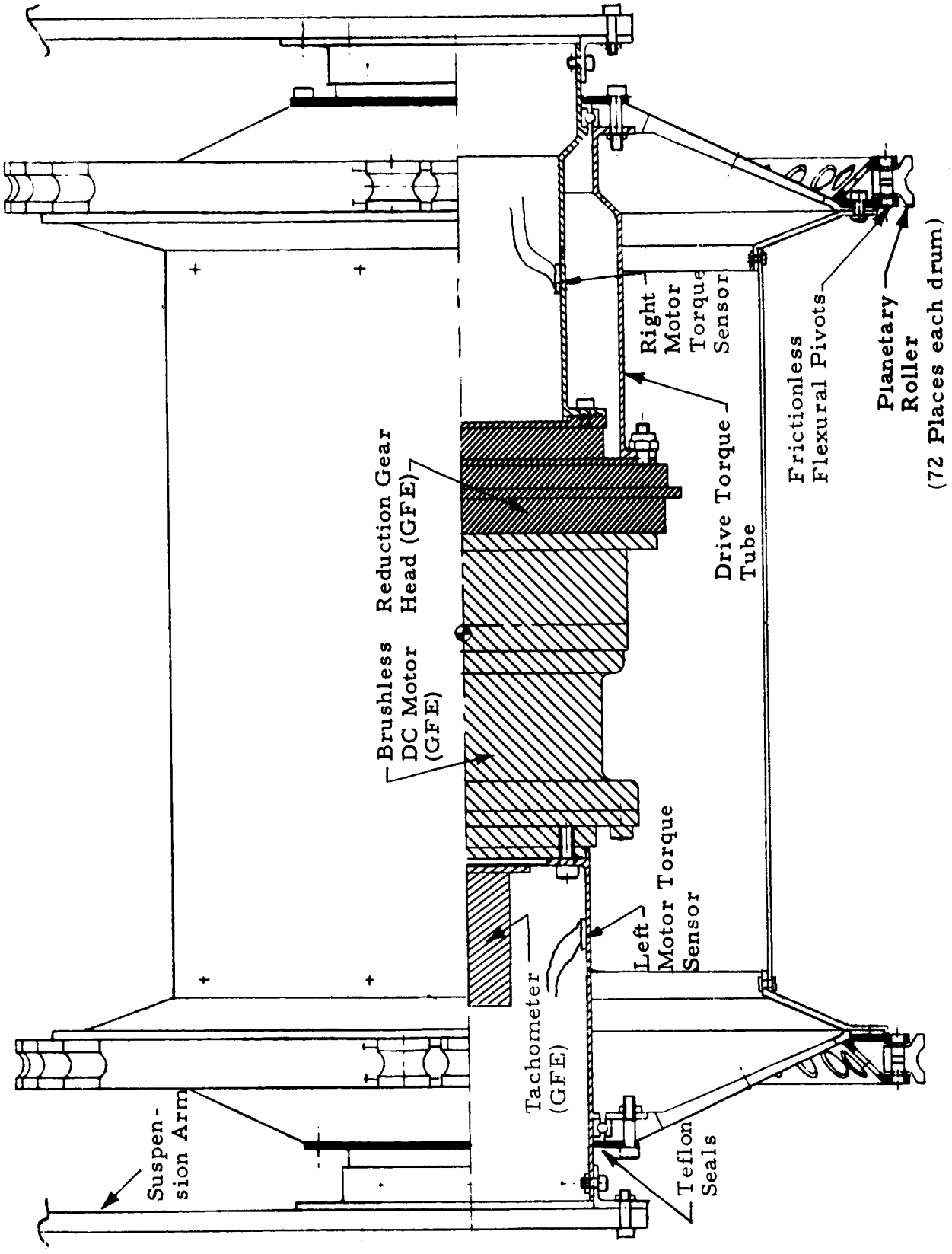

Fig. 6 - Layout of Drive Motor Installation and Drive Torque Sensor Locations

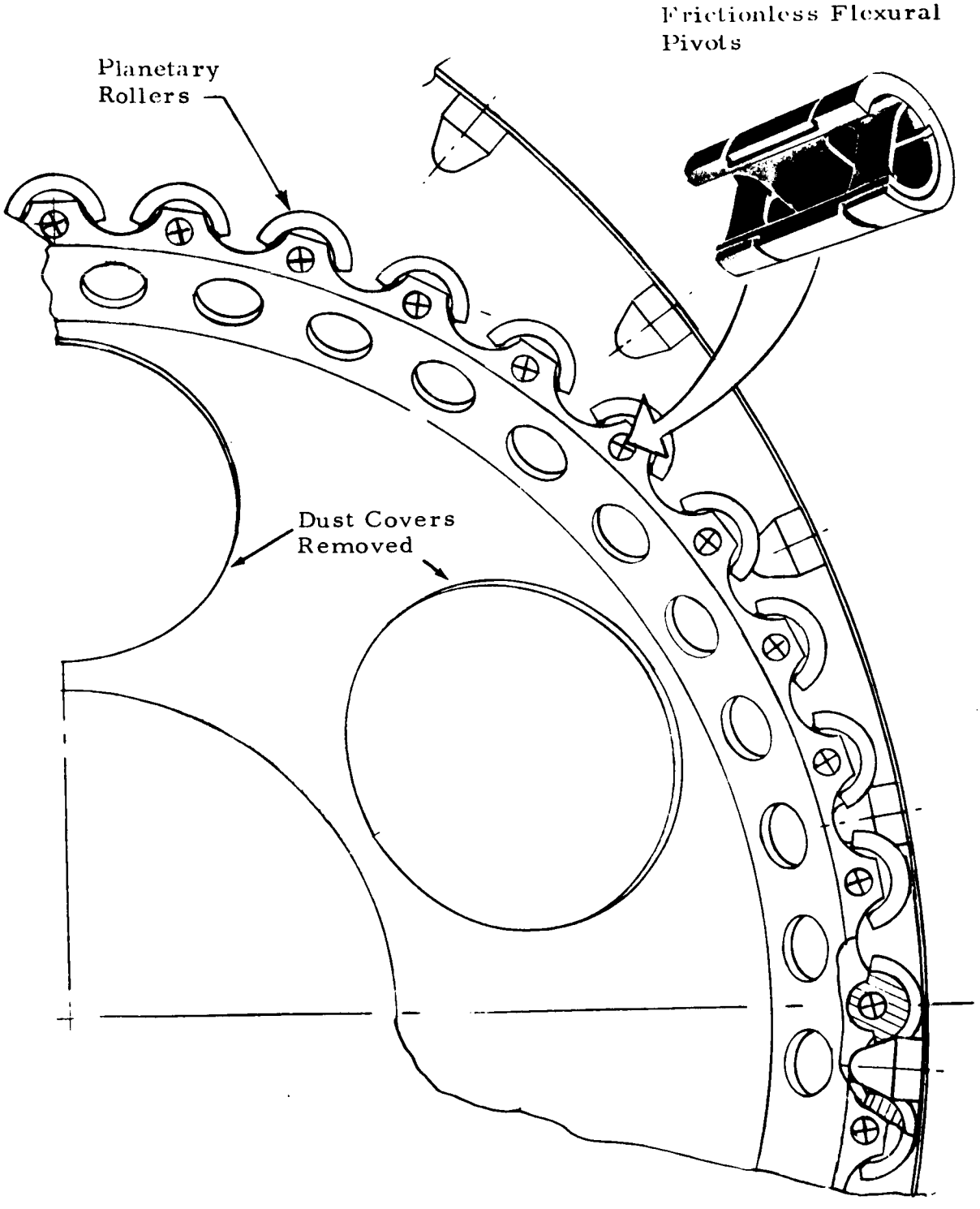

Fig. 7 - Sideview of Drive Drum, Planetary Rollers and Flexural Pivots for Frictionless Mounting of Rollers

the roller bearings. They provide ±12 degrees of rotary motion for rolling contact during engaging and disengaging of the drive lugs, exceeding the predicted deflections by a wide margin.

2.3 INSTALLATION OF LARGE GROUSERS FOR IMPROVED TRACTION

The redesigned elastic loop and the associated new forming concept results in almost straight lower edge sections as shown in Fig. 2a. This permits the installation of large grousers that provide near uniform ground pressure across the complete width of the loop as shown in Fig. 8.

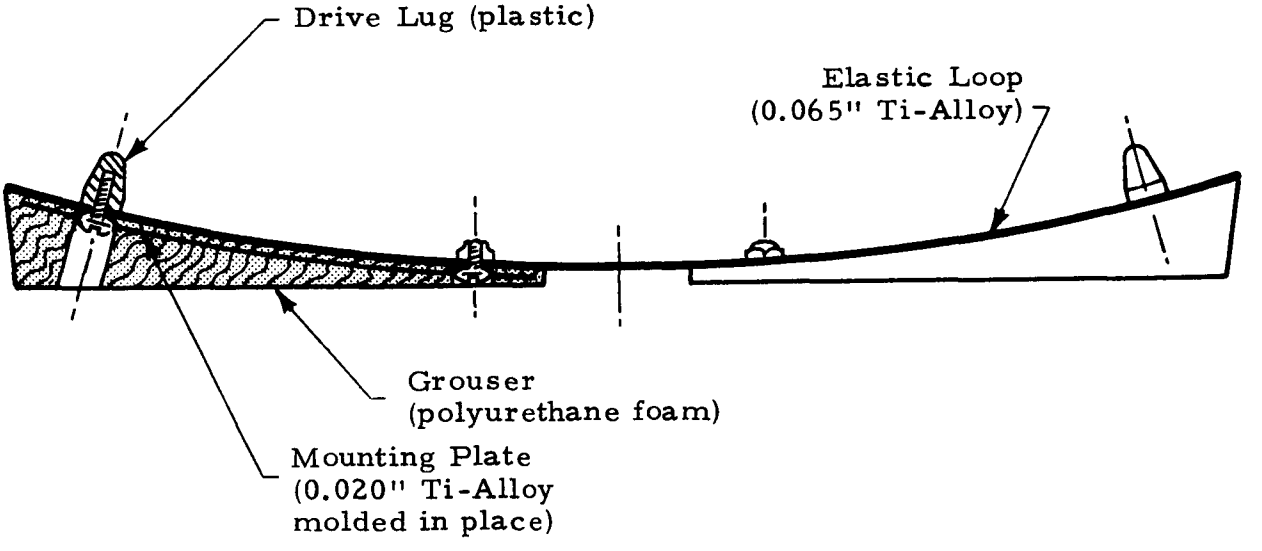

Fig. 8 - Cross Section of Elastic Loop Segment in Contact with Ground (Lightweight foam grousers provide near-constant contact pressure across loop width.)

For lightweight and sufficiently soft spring characteristics under the expected low contact pressures below 0.7 N/cm^2 (1 psi), polyurethane foam was selected as grouser material. To ensure safe and simple mounting and to enhance the structural integrity of the grousers, a thin titanium-alloy mounting plate with two mounting holes is molded into each grouser. The outer mounting bolts are also used to hold the drive lugs so that a minimum number of holes is drilled into the elastic loop.

2.4 ADJUSTABLE SHOCK ABSORBERS TO OPTIMIZE ELMS DAMPING CHARACTERISTICS

Two lightweight adjustable shock absorbers have been fabricated and installed between the ELMS chassis and the drive drum support arms to damp the motion of the ELMS unit in excessive pitching or vertical oscillations and to absorb horizontal impact loads. The front shock absorber is visible in Fig. 2a. The damper design is shown in Fig. 9. One-way damping action is required to assure continuous contact and drive torque transmission between loop and drive drums during outward deflections of the drums.

Energy dissipated in the shock absorbers can be monitored by measuring the piston force F and the piston travel s using an on-board strain gaged clevis for each damper and potentiometers which have been installed inside the ELMS chassis. Dissipated energy E is then obtained by integrating

$$E = \int F ds$$

over the duration of the test.

2.5 SUPPORT TRAILER FOR MULTI-MODE TESTING

The results from the single-loop ELMS test program should enable worst-case predictions of major performance characteristics during slope climbing and negotiation of typical obstacles. The lateral support and instrumentation required for the performance of actual slope climbing and obstacle negotiation tests using a single ELMS unit could be provided, in a simple manner, by a lightweight trailer. The trailer was designed to simulate the interactions of a second articulated ELMS module connected to the front unit as realistically as possible.

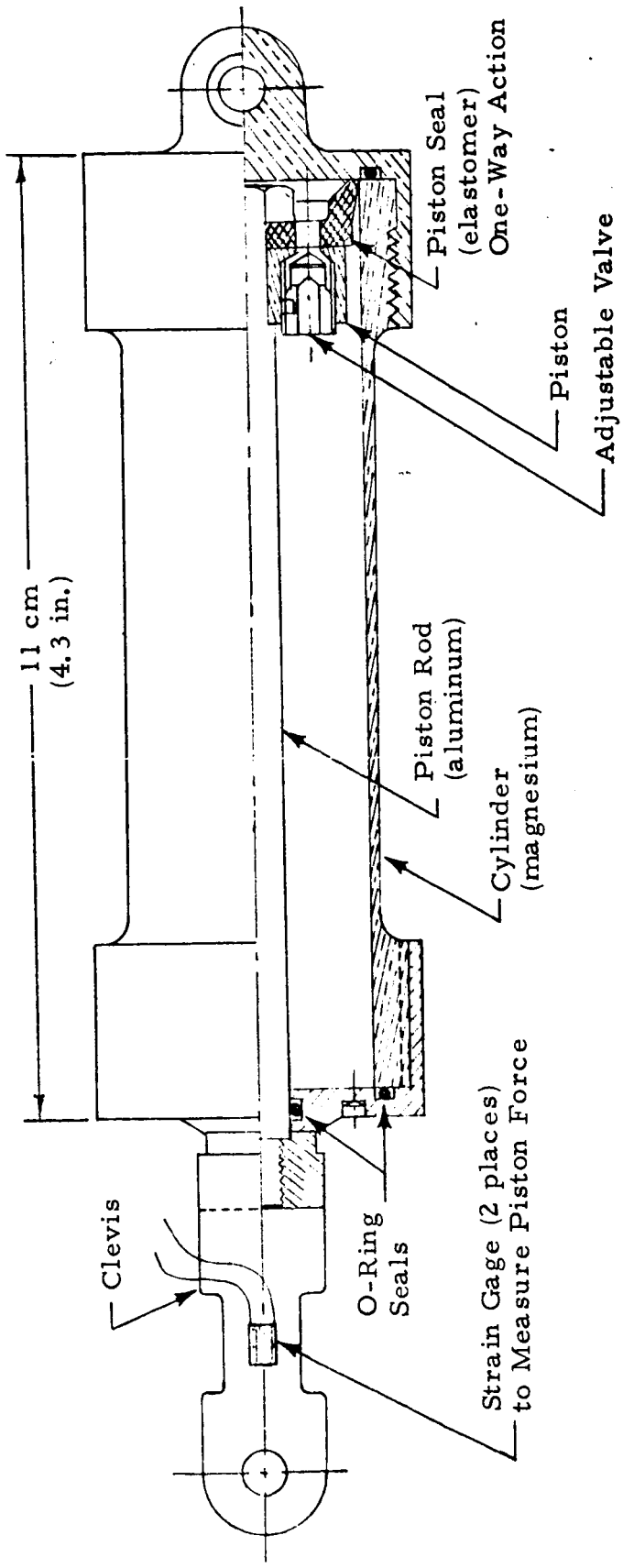

Fig. 9 - Lightweight Adjustable Shock Absorber Layout
(Two shock absorbers damp ELMS test unit in
pitch and in vertical oscillations).

The major configurations which were considered for simulation by the support trailer are shown in Fig. 10. The trailer has four functions when the ELMS unit is operated in an autonomous remotely controlled mode:

1. Simulating the major load interactions of a second ELMS module in tandem with the present ELMS test unit;
2. Carrying instrumentation that cannot be mounted onboard (such as pull sensors, pitch torque sensors, odometer);
3. Generating an adjustable amount of drag or drawbar pull;
4. Offsetting any weight of the ELMS in excess of the desired test load, if the test load is below the ELMS 1-g weight.

In analyzing the various joint designs and load interactions of the configurations shown in Fig. 10 it was found that all cases result in basically one of three pitching modes at the articulated pitch joint:

- Locked in Pitch
- Spring Restrained in Pitch
- Free in Pitch

The trailer design which provides all three pitching modes at lightweight and little complexity is shown in Figs. 11 and 12. Locking in pitch is achieved by rigid turnbuckle connections of the upper tubes which allow for pitch angle adjustment. Replacing the rigid connections by a pair of coil springs results in the spring restrained pitching mode. Free pitching is accomplished by using again the rigid connections of the upper tubes but allowing the outer transverse tubes (A) to rotate freely (between adjustable hard stops) about the transverse smaller tube (B).

A dry particle electromagnetic brake (Figs. 12 and 13) transmits variable torques to the trailer wheels which are mounted on a common axle.

1. SINGLE PITCH JOINT ARTICULATION

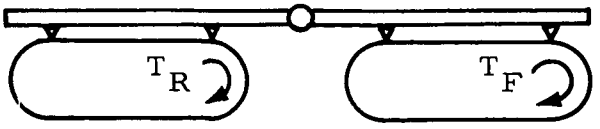

1a. For equal drive torques ($T_R \approx T_F$) on flat terrain acts approximately like locked in pitch.

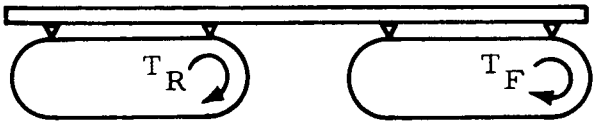

1b. If one unit is under power only, both units act like spring restrained in pitch.

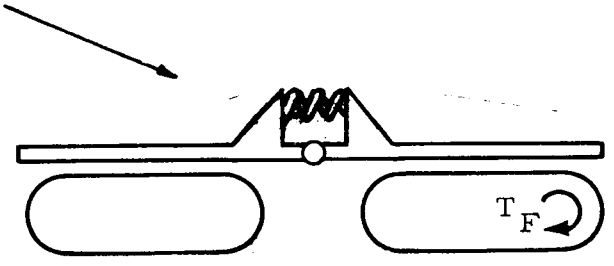

2. DUAL PITCH JOINT ARTICULATION (Rear joint or all joints may have positive pitch control)

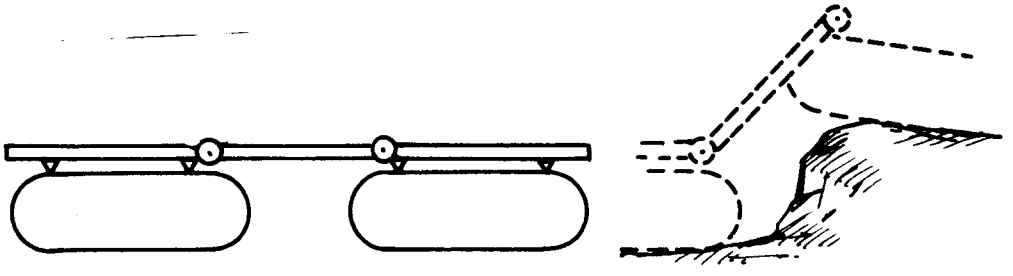

2a. Joints passive: Free pitching for both units.

2b. Joints pitch controlled: Both units locked in pitch (acts like 1a)

3. FLEXIBLE FRAME (identical to 1b)

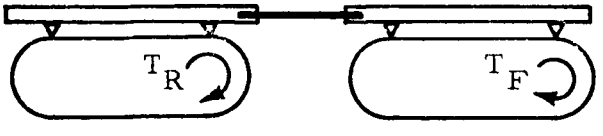

Fig. 10 - Major Dual-Unit ELMS Pitch Joint Configurations Considered in the Design of ELMS Support Trailer

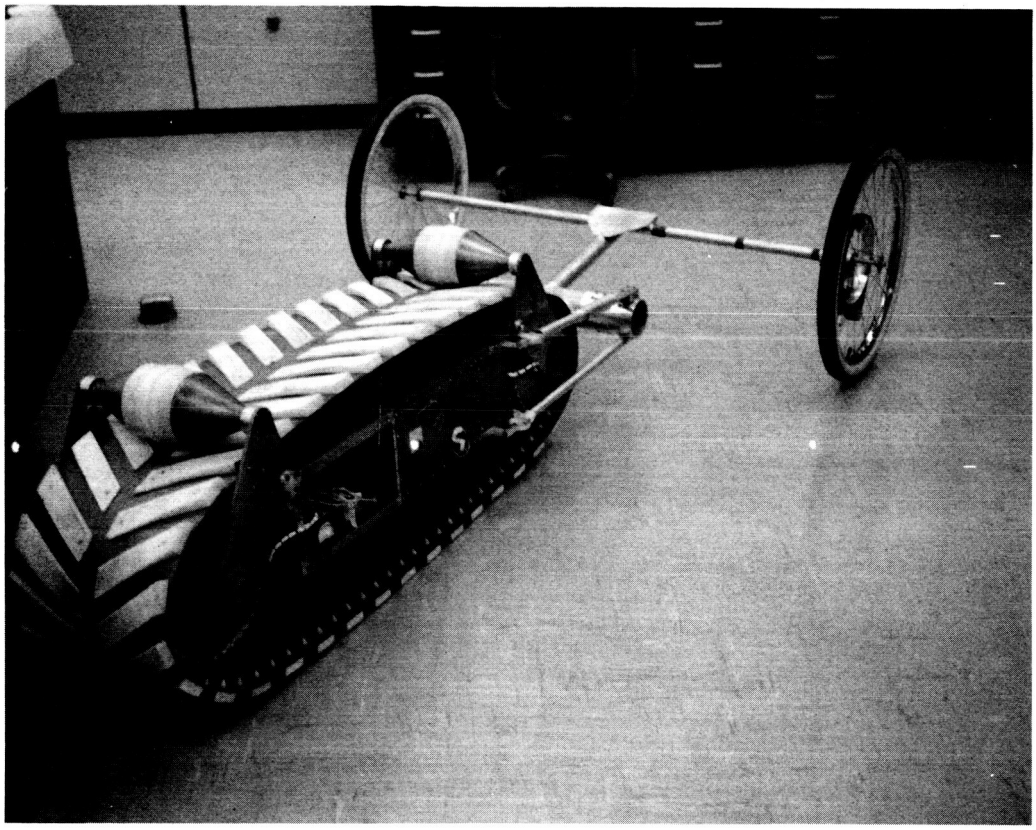

Fig. 11 - ELMS Test Unit and Support Trailer

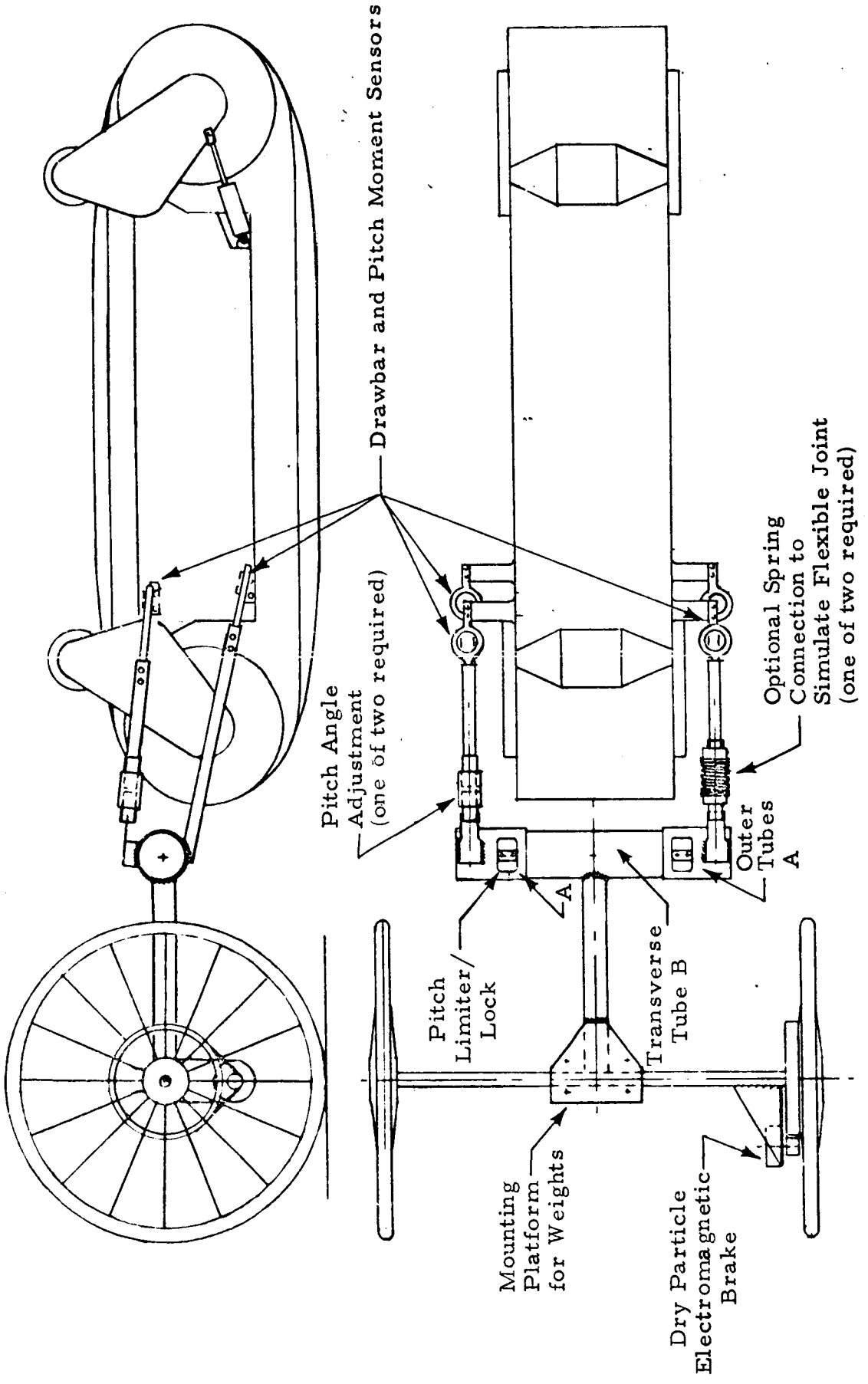

Fig. 12 - ELMS Trailer for Stabilization, Measurement of Drawbar Pull, Pitch Torques, Vehicle Speed and Travel and for Generating Specified Drag

Fig. 13 - Dry Particle Electromagnetic Brake Generates Calibrated Drawbar Pull. Continuous Turn Potentiometer for Measurement of Distance

Four ring shaped strain gaged sensors measure drawbar pull and pitch torque transmitted from the trailer to the ELMS test unit at the four attachment points as shown in Figs. 11 and 12.

2.6 INSTRUMENTATION FOR ELMS PERFORMANCE EVALUATION

The ELMS test unit built under this contract has been extensively instrumented for measuring all primary parameters necessary for a thorough performance evaluation in an unambiguous manner. Table 2 summarizes quantities to be measured according to the contract, Exhibit A, Section II B, and the selected instrumentation. In order to simplify interfacing with the WES test facility and calibration, several WES-owned instruments are furnished GFE during the performance evaluation test program as indicated in the table.

Table 2

MEASURED PARAMETERS AND SELECTED INSTRUMENTATION FOR ELMS PERFORMANCE EVALUATION

Item	Required Parameter (P_R)	Measured Parameter(s) (P_M)	Relationship $P_R=f(P_M)$	Instrumentation Selected	Shown in Figure	Remarks
a	Input Drive Torque M_{IN}	1. Motor Current I and Angular Velocity ω_D	$M_{IN}=f_1(I, \omega_D)$	Motor Calibration Charts	Vol. II, Figs. 7-6 and 7-7	
		2. Strain ϵ_a in Motor Supports	$M_{IN}=f_2(\epsilon_a)$	Straingaged Motor Support Tubes	6	
b	Angular Velocity of Drums, ω_D	Tachometer Voltage V_c	$\omega_D=C_c V_c$	Tachometers	6	
c	Input Energy, E_{IN}	1. Electrical Input Energy; Battery Current Battery Voltage	$E_{IN}=\int Vdt$	Amp-Meter Volt-Meter		
		2. Mechanical Input Energy; $M_{Drum};\omega_D$	$E_{IN}=M_D\omega_D$	See Items a, b		
d	Drawbar Pull, P	Strain ϵ_d in 4 Trailer Arms	$P=\Sigma C_d \epsilon_d$	Straingaged ring sensors	12	
e	Translational Speed, v	Trailer/Carriage Tachometer Voltage V_b	$v=C_b V_b$	Tachometers	6 and 13	Drive pulley and belt furnished by Lockheed; Tach. GFE by WES
f	Output Energy, E_{OUT}	P, v	$E_{OUT}=Pv$	See Items d, e		
g	Efficiency, η	$E_{IN};E_{OUT}$	$\eta=E_{OUT}/E_{IN}$	See Items c, f		
h	Slip, S	Drum Angular Velocity ω_D; v; rolling radius r_c	$\text{Slip}=\frac{\omega_D r_c - v}{\omega_D r_c}$	See Items b, e	13 and 6	Alternate Method: String Pay-Out Instrumented with Load Cell
i	Traction-Drive Energy Requirements, ΔE	E_{IN}, E_{OUT}	$\Delta E=E_{IN}-E_{OUT}$	See Items c, f		
j	Internal Energy Losses, E_{INT}	E_{IN}, E^*_{OUT}, (Loop on Rollers, Lifting Weight)	$E_{INT}=E^*_{OUT}-E_{IN}$	ELMS on Frictionless Rollers; String and Pulley Arrangement to Lift Weight		
k	Dissipated Damper Energy, E_d	1. Strain in Piston Rod	Piston Force: $F=C_{k1}\epsilon_k$	Straingaged Clevises	9	
		2. Potentiometer Voltage	Piston Travel $S=C_{k2}V_k$; $E_d=\int Fds$	Potentiometers	Vol. II Fig. 7-8	
ℓ	Contact Pressure Distribution, p	Output Voltage V_ℓ of Pressure Transistors	$p=f(V_\ell)$	"Pitran" Pressure Transistors mounted in special grouser	14	
m	Pitch Torque, M_p	Strain in 4 Trailer Arms (as in "d")	See Item f,2 $M_p=h(P_{Top}-P_{Bot})$	Straingaged Ring Sensors	12	
n	Trailer Drag P_T	Brake Current I_n	Brake Torque $M_n=f(I_n)$; $P_T=M_n/r_c$	Dry Particle Electric Brake	12;13	

In addition to the 70 grousers mounted on the elastic loop, a special grouser was fabricated with instrumentation to measure ground pressure distribution between grousers and the soil. A layout is shown in Fig. 11. Pressure-sensitive transistors have been found to be the most compact pressure sensors available. Small size is important to minimize the increase of grouser spring stiffness under load.

All instrumentation installed on board the ELMS test unit and support trailer has been checked out and calibrated before delivery. A detailed description of the sensors and all calibration data are given in Volume II.

2.7 REMOTE CONTROL AND DATA TELEMETRY SYSTEMS INSTALLATION

Sufficient weight and space allocations have been made to permit installation of a remote control unit and data telemetry system in the front bay of the ELMS chassis as shown in Fig. 12. A reinforced mounting base of 13 cm x 38 cm area is available to hard mount this equipment. Antenna installation and associated feedthroughs can readily be accommodated near that mounting base.

Removable panels provide ready access to all onboard equipment, including drive motor wire outlets, tachometers, torque sensing strain gages, battery, drive motor controllers, potentiometers to measure shock absorber piston travel and the remote control and telemetry units provided GFE by WES.

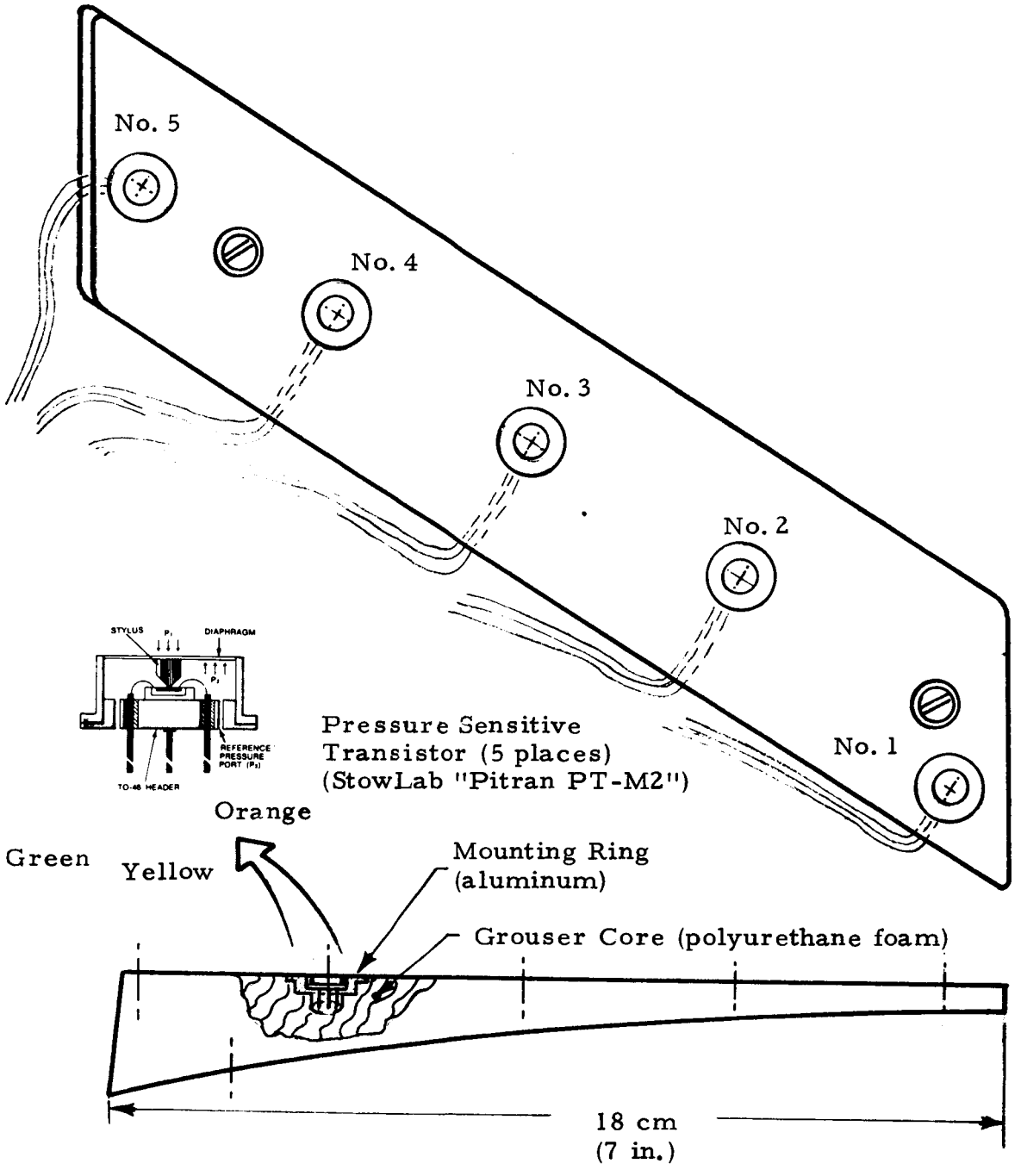

Fig. 14 - Instrumented Grouser for Measurement of Ground Pressure Distribution Across Half of the Loop Width

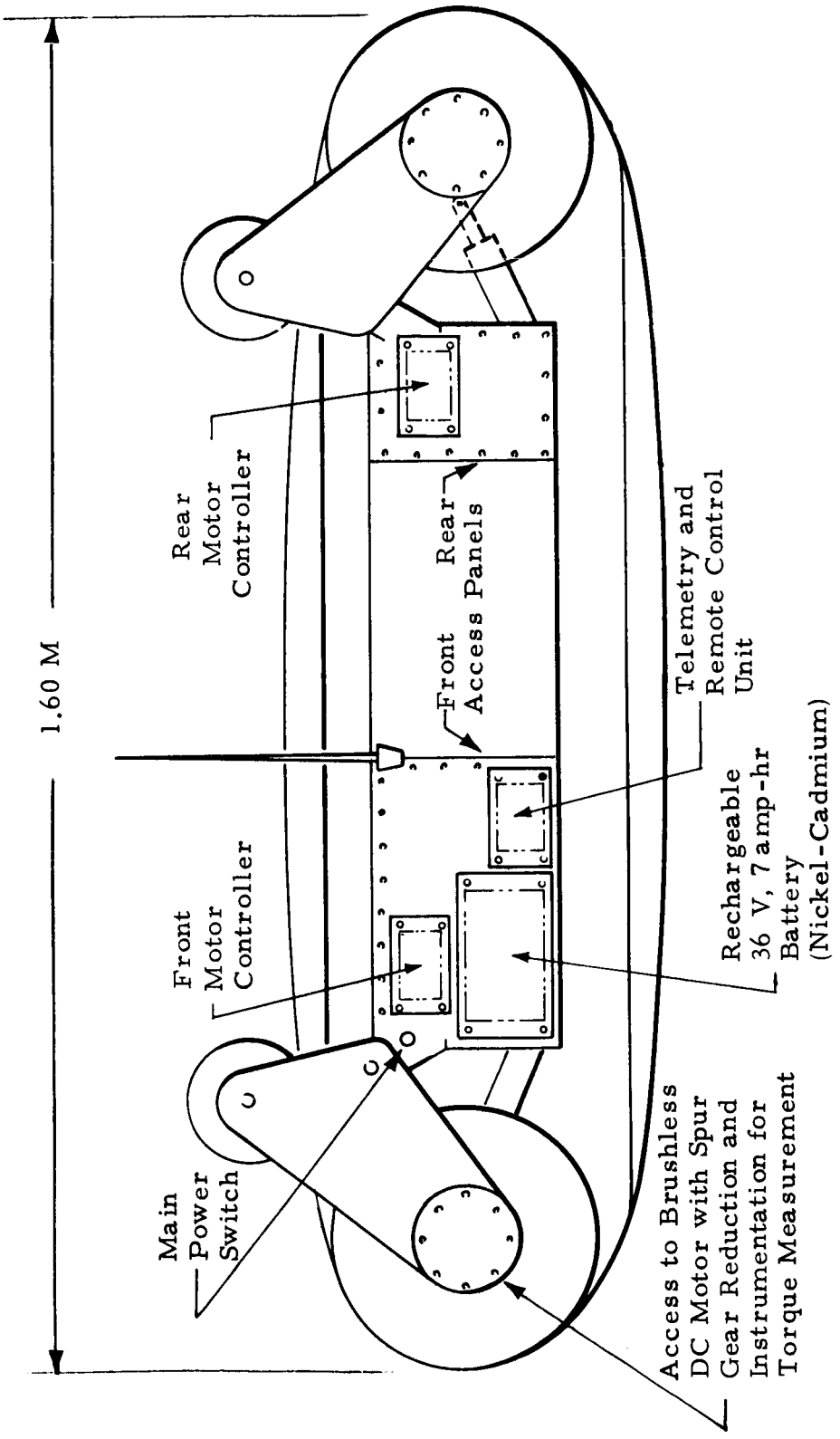

Fig. 15 - Location of and Accessibility to Major Subsystems Including Remote Control and Telemetry Units

Section 3
PRELIMINARY RESULTS FROM ELMS ACCEPTANCE TEST PROGRAM AT WES

Upon delivery of the second-generation ELMS to MSFC an acceptance test program was conducted at the U. S. Army Engineer Waterways Experiment Station (WES) in Vicksburg, Mississippi, under NASA-Defense Purchase Request No. H 87478A during the period 9 June to 13 July 1972.

For a first assessment of the ELMS performance characteristics the preliminary results of these acceptance tests were made available for publication in this report through the courtesy of Dr. N. C. Costes of MSFC's Space Sciences Laboratory.

The purpose of the tests was to verify the structural integrity of the ELMS and the proper functioning of its instrumentation, and to assure the compatibility of the test unit with the WES test facility.

The three types of acceptance test conditions are summarized in Table 3. The tests on level surface (test series "a") were performed in the WES single-wheel dynamometer system. A special support had been built to mount the ELMS in a test carriage for programmed slip tests in a lunar soil simulant (LSS) similar to the first-generation tests reported in Ref. 2. The same dynamometer facility had been used extensively in previous tests of Lunar Roving Vehicle (LRV) wheels as used during the Apollo 15 and 16 missions (Refs. 7, 8, 9 and 11). ELMS test results therefore lend themselves to direct comparisons with performance data of LRV-wheels and of the first-generation ELMS. Slope climbing tests (series "b" in Table 3) are performed with the ELMS in its autonomous remote-controlled mode where the two-wheeled passive support trailer provided vehicle stabilization. Natural soft-soil slope conditions were achieved by tilting a large soil bin filled with crushed bassalt of specified soil consistency to the desired slope angle. In addition

Table 3

ACCEPTANCE TEST CONDITIONS FOR SECOND GENERATION ELMS, JUNE 1972 AT WES, VICKSBURG, MISSISSIPPI

(a) Single Unit Tests on Level Surface (Two-Pass Tests)

Test No.	Soil Type	ELMS Speed m/sec	Slip Condition	WES Damper	Pitch Angle deg
72-001-6	LSS_2	0.5	CPS*	ON	FREE
002-6	LSS_1	0.5	"	ON	0
003-6	LSS_1	2.0	"	OFF	4
004-6	LSS_3	2.0	"	ON	0
005-6	LSS_2	0.5	"	OFF	0
006-6	LSS_2	2.0	"	ON	0

(b) ELMS-Trailer Tests on Slopes

Test No.	Pass No.	Soil Type	ELMS Speed m/sec	Slip Condition	Slope Angle deg	Equiv. Slope w/o Trailer deg	Remarks
007-6	1	LSS_1	≈0.5	CPS*	0	0	
	2	LSS_1	≈0.5	CPS	0	0	
008-6	1	LSS_1	≈0.2-0.6	FD**	25	30	go
	2	LSS_1	0.5	CPS	25	30	
009-6	1	LSS_1	≈0.2-0.6	FD	28	33	Immobilized (100% slip)
	2	LSS_1	≈0.03-0.2	FD	27	32	go

(c) ELMS-Trailer Tests on Obstacles

Test No.	Pass No.	Soil Type	ELMS Speed m/sec	Slip Condition	Obstacle Type	Obstacle Heights cm	Remarks
010-6	1	Hard Surface	creep	FD	Rigid Step	25	go
	2	"	"	"	"	31	go
	3	"	"	"	"	38	go, but restrained by maximum pitch possible
	4	"	"	"	"	46	go, free trailer pitch, but restrained by center tube of trailer, which touched the ground

* Classical programmed slip test. ** Freely developed.

to its own weight of 670 N (151 lb), the ELMS had to pull the weight of the trailer of 139 N (31 lb) up the slope. The maximum slope of 27 degrees (test No. 009-6) which was climbed by the ELMS connected to the trailer is equivalent to a 32 degree slope without trailer. This is in agreement with ELMS scale-model tests recently conducted at the Space Sciences Laboratory's wheel-soil interaction test facility under the direction of Dr. N. C. Costes, where a 1/6-scale model of the second-generation ELMS also climbed slopes up to 32 degrees under the same soil conditions.

The third series of tests (test No. 010-6 in Table 3) involved obstacle negotiation.

Step-obstacles of increasing step height up to 46 cm (18 in.) were negotiated which is equal to the total height of the elastic loop under nominal load. A multi-loop roving vehicle such as the articulated configuration of Fig. 1 can be expected to climb substantially higher obstacles.

Typical results of a programmed slip test on level ground (test No. 005-6) are plotted in Fig. 16 and 17 and can be compared with the first-generation ELMS (Ref. 2) and with the Boeing-GM LRV-wheel performance (Ref. 8) for the same soil condition (LSS_2).

A dramatic improvement in tractive capability over both ELMS I and LRV is indicated in Fig. 16, where the ratio drawbar pull/weight is plotted over slip. Very high traction ($P/W > 0.6$) is achieved at remarkably low slip values of less than 15% which keeps energy losses at the loop-soil interface small. The LRV-wheel requires substantially higher slip conditions to develop high drawbar pull.

In earlier studies and tests (Ref. 7) it had been verified for light loads and low to medium slope angles that P/W measured on a level surface for a single wheel is roughly equivalent to the tangent of the slope that a vehicle equipped with such wheels can climb. This slope angle $\alpha \approx \tan^{-1} P/W$ is therefore included as an additional scale.

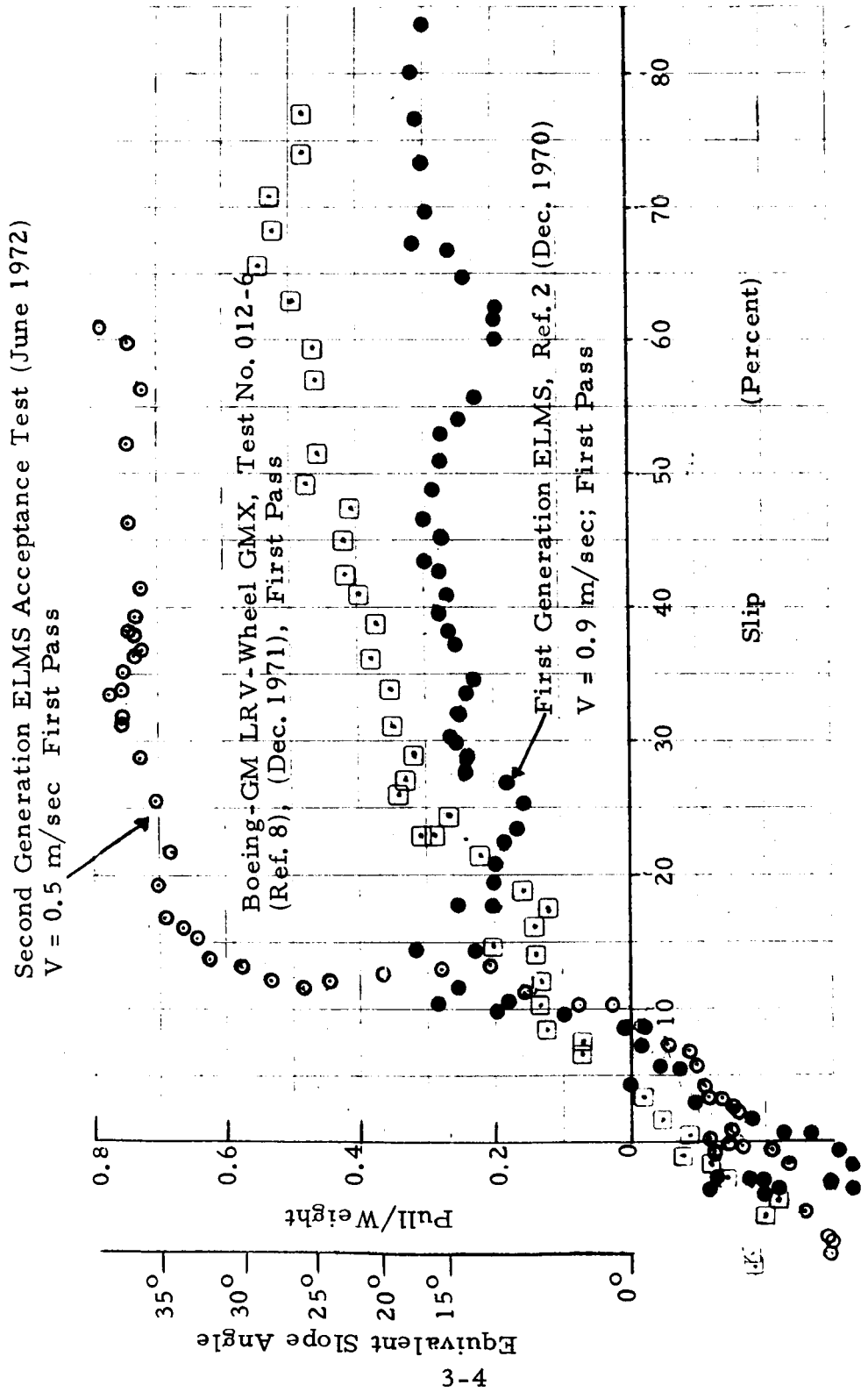

Fig. 16 - Preliminary Results of Typical Acceptance Test (No. 72-005-6) on Level Surface for Second-Generation ELMS (●) Compared with Boeing-GM LRV-Wheel Performance (⊡) and First-Generation ELMS (●) in Same Test Facility and Soil Condition (Lunar Soil Simulant No. 2)

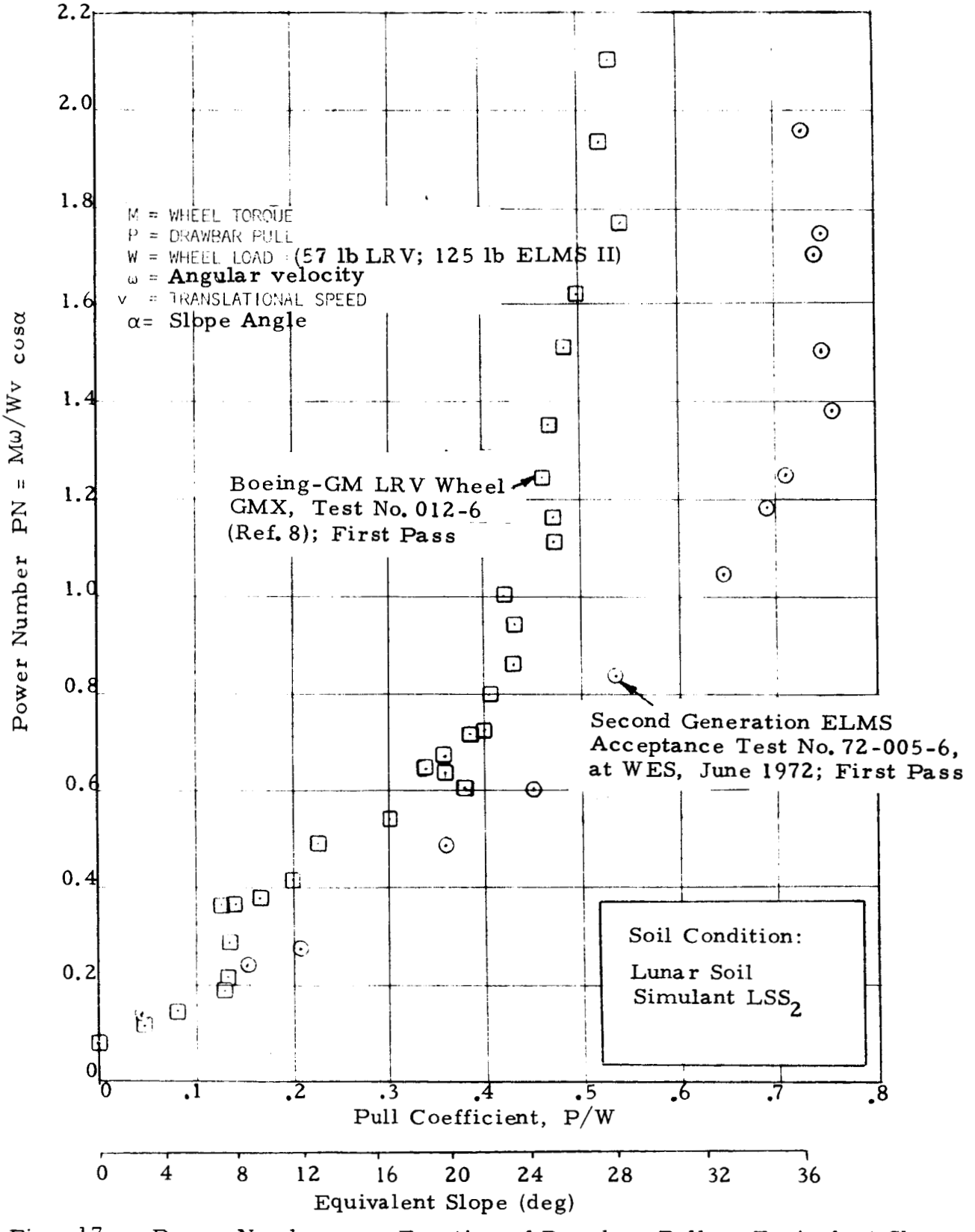

Fig. 17 - Power Number as a Function of Drawbar Pull or Equivalent Slope for Second Generation ELMS and for Boeing-GM LRV-Wheel

While tracked vehicles have been known for superior soft-soil traction their complex mechanical design traditionally caused much higher internal losses so that overall power requirements far exceed those of wheeled vehicles. However, the greatly simplified "track" configuration of the ELMS with an endless elastic loop and a minimum of moving parts for its support (no bogie-wheels) result in lower overall power requirements for all slope angles above 7 degrees when the second-generation ELMS is compared with the Boeing-GM LRV-wheel for the same soil condition as plotted in Fig. 3-2. The power number PN is defined as

$$PN = M\omega/Wv \cos\alpha$$

where M is wheel or drive drum torque, ω is wheel or drum angular velocity in rad/sec, W is weight and v is vehicle translational speed and α is the slope angle. This dimensionless power number represents the energy consumed per unit of distance traveled and per unit load acting normal to the surface traversed by the vehicle.

According to these tests performed in the same dynamometer and under the same soil conditions, the second-generation ELMS requires less than 75% of the energy of the wire mesh wheel for slopes above 8 degrees and is about equal in energy requirements on level or near-level ground.

Section 4
SUMMARY AND CONCLUSIONS

Several significant design improvements have been incorporated into the second-generation full-scale ELMS test unit which was built under this contract for the first time following earlier successful small-scale model experiments. A major improved design accomplishment was the increase of the load carrying capacity of elastic loops without severe weight or stress penalties. Redesign of the loop form and size, plus selection of a more advanced titanium alloy, resulted in performance characteristics representing a marked improvement over the first-generation unit, as shown below in Table 4.

Table 4

COMPARISON OF MAJOR DESIGN CHARACTERISTICS OF FIRST AND SECOND GENERATION ELASTIC LOOPS

	Design Load F_o	ELMS Weight (w/o Battery)	Available Spring Deflection at F_o	Stress Ratio σ/σ yield at F_o	Effective Footprint at F_o	Total Available Drive Torque
1st Generation Elastic Loop	253 N (57 lb)	380 N (86 lb)	7 cm (2.7 in.)	0.45	1080 cm^2 (174 in^2)	41 Nm (30 ft-lb)
Present Elastic Loop	530 N (120 lb)	420 N (95 lb)	13 cm (5 in.)	0.42	1970 cm^2 (317 in^2)	81 Nm* (60 ft-lb)
Change (%)	+110	+11	+86	- 7	+82	+100

*GFE Brushless DC-motors capable of 217 Nm (160 ft-lb) total torque have been limited to maximum torque required for ELMS testing [expected to be 81 Nm (60 ft-lb)].

Another important design improvement was the shaping of the loop's footprint into a favorable form for uniform pressure distribution. The new loop form resulting from a combination of bulge-forming and roll-forming permits the installation of large grousers for increased contact area and improved traction. No such grousers could be mounted on first-generation loops formed by roll-forming only.

Other design improvements are associated with a more efficient drive torque transmission from the internal drive drums to the elastic loop which are expected to reduce the internal losses of the drive system.

The new ELMS test unit is built for testing in the WES mobility test facility and for autonomous remotely controlled operation under battery power. A support trailer has been built which will simulate a second ELMS module in tandem operation. An additional purpose of the trailer is to serve as a fifth wheel, to provide drag, if required, and to house other instrumentation for performance testing.

The main problems encountered during this program were encountered in the manufacture of elastic loops with specified shape and spring characteristics under load. Manufacturing techniques which had resulted in satisfactory loops in earlier small-scale tests using a standard titanium alloy (Ti-6Aℓ-4V) were found impractical when scaled up and applied to advanced titanium alloys because they required heat treatment after forming. These manufacturing problems delayed completion of the unit and caused minor irregularities in the loop's elastic characteristics. A hot-forming technique has been identified as the technique best suited to manufacture future loops using advanced state-of-the-art titanium alloys. However, the irregularities of the present loop are not expected to have appreciable adverse effects on the performance of the ELMS test unit as indicated by the preliminary test results of the acceptance test program performed at WES, and by ELMS model tests performed at the Geotechnical Research Laboratory of the MSFC Space Sciences Laboratory under Contract NAS8-28437.

The new ELMS unit will be capable of being integrated, on a modularized basis, with a multi-loop articulated ELMS test vehicle as the next logical step in the development of this mobility concept.

Section 5
REFERENCES

1. Posnansky, H. A., "Self-Supporting Track," Disclosure of Invention No. D-03-5465, Lockheed Missiles & Space Company, Huntsville, Ala., 1969.

2. Melzer, K.-J., and A. J. Green, "Performance Evaluation of a First-Generation Elastic Loop Mobility System," TR-M-71-1, U. S. Army Engineer Waterways Experiment Station, Vicksburg, Miss., May 1971.

3. Costes, N. C., W. D. Carrier, J. K. Mitchell, and R. F. Scott, "Apollo 11 Soil Mechanics Investigation," NASA SP-214, Sec. 4, Apollo Preliminary Science Report, 1969.

4. Scott, R. F., W. D. Carrier, N. C. Costes, and J. K. Mitchell, "Mechanical Properties of the Lunar Regolith - Apollo 12 Preliminary Science Report," NASA SP-235, 1970, pp. 161-188.

5. Costes, N. C., G. T. Cohron, and D. C. Moss, "Cone Penetration-Resistance Test — An Approach to Evaluating the In-Place Strength and Packing Characteristics of Lunar Soils," Proc. of the Second Lunar Science Conf., Vol. 3, 1971, pp. 1973-1987.

6. Mitchell, J. K., L. G. Bromwell, W. D. Carrier, N. C. Costes, and R. F. Scott, "Soil Mechanics Experiment," NASA SP-272, Sec. 4, Apollo 14 Preliminary Science Report, 1971.

7. Freitag, D. R., A. J. Green, K.-J. Melzer and N. C. Costes, "Wheels for Lunar Vehicles," Proceedings of Off-Road Mobility Symposium, International Society for Terrain Vehicle Systems (ISTVS) - TRW Systems, El Segundo, Calif., 1970.

8. Green, A. J., and K.-J. Melzer, "Performance of the Boeing LRV Wheels in a Lunar Soil Simulant; Effect of Wheel Design and Soil," TR M-71-10, Report 1, U. S. Army Engineer Waterways Experiment Station, Corps of Engineers, Vicksburg, Miss., 1971.

9. Melzer, K.-J., "Performance of the Boeing LRV Wheels in a Lunar Soil Simulant, TR M-71-10, Report 2, U. S. Army Engineer Waterways Exe Experiment Station, Corps of Engineers, Vicksburg, Miss., 1972.

10. Mitchell, J. K., R. F. Scott, W. N. Houston, N. C. Costes, W. D. Carrier, and L. G. Bromwell, "Mechanical Properties of Lunar Soil: Density, Porosity, Cohesion, and Angle of Internal Friction," Proceedings, Third Lunar Science Conference, Houston, Texas, 10-13 January 1972.

11. Costes, N. C., J. E. Farmer, E. B. George, "Mobility Performance of the Lunar Roving Vehicle Terrestrial Studies – Apollo 15 Results," Proceedings of the 4th International Conference of the International Society for Terrain-Vehicle Systems, Stockholm, Sweden, 1972.

12. Mitchell, J. K., L. G. Bromwell, W. D. Carrier, N. C. Costes, W. N. Houston, and R. F. Scott, "Soil Mechanics Experiment – Apollo 15 Preliminary Science Report," NASA SP 289, Chapter 7, 1972.

13. Lessem, A. S., "Operations and Maintenance Manual for a Scale-Model Lunar Roving Vehicle," Misc. Paper M-72-3, U. S. Army Engineer Waterways Experiment Station, Corps of Engineers, Vicksburg, Miss., April 1972.

14. Trautwein, W., "Elastic Loop with Uniform Longitudinal Ground Pressure Distribution," Disclosure of Invention No. D-03-5917, Lockheed Missiles & Space Company, Huntsville, Ala., 3 May 1971.

15. Technical Proposal, "Produce an Improved Single Elastic Loop Mobility System and Submit for Testing," LMSC-HREC D225075, June 1971.

16. Chang, J. C., "Fabrication Study of Beta III Titanium Alloy Sheet and Foil," WESTEC Paper W 71-23.1, Los Angeles, Calif., March 1971.

17. Jones, C. S., Jr., B. J. Doran, F. J. Nola, "Traction Drive System Design Considerations for a Lunar Roving Vehicle," NASA TMX-53972, November 1969.

18. Jones, C. S., Jr., and F. J. Nola, "Mobility Systems Activity for Lunar Rovers at MSFC," NASA TMX-64623, September 1971.